Commutation Torque Ripple Reduction for Direct DC-link Current Control by Applying Multilevel Hysteresis Controller and Proper Voltage Vectors

R. Heidari[1], K.-I. Jeong[1], and J.-W. Ahn[1]
[1] Department of Mechatronics Engineering, Kyungsung University, Busan, South Korea

***Abstract*-- To achieve high-performance control of the brushless direct current (BLDC) motors, a direct DC-link current control (DDLCC) is introduced and compared with the direct torque control (DTC) method. Similar to the DTC method, the proposed DDLCC method has a fast transient response; nonetheless, it comes with higher reliability, cost-effectiveness, and lower torque ripple. Although this method provides average torque ripples lower than those of the DTC method, the commutation torque ripple is higher. A four-level hysteresis controller is utilized to distinguish the commutations, and then, the commutation torque ripple is suppressed by applying appropriate voltage vectors. These vectors provide similar fall time and rise time for both commutated currents and suppress commutation torque ripple. The results verify these appropriate voltage vectors guarantee the stable performance of the BLDC motor as well as commutation torque ripple reduction compared to the conventional DTC method.**

***Index Terms*—BLDC motor, commutation torque ripple, multilevel hysteresis controller, voltage vectors.**

I. Introduction

The trapezoidal-based BLDC motors have drawn many manufacturers' attention to use for their products owing to their high efficiency, cost-effectiveness, power density, and simple control [1]. These types of motors are back-EMF-based, and each phase should conduct during the top flat part of back-EMF voltage with a constant current. That is, two phases conduct every 60 electrical degrees [2].

In general, the torque ripple of BLDC motors is higher than that of PMS motors owing to stator teeth, variable reluctance, and current commutation [3]. To face these problems, the scholars have introduced techniques like inserting the stator winding inside the stator closed slots [4], applying a magnetic screen in the rotor core [5], controlling the DC-link voltage by the DC-DC converters [6], modifying the control of BLDC motors [7-10].

Hysteresis-based methods are usually performed on these types of motors [7]. Reducing both commutation torque ripple and average torque ripple is the main target of these techniques. For example, hysteresis current control is applied to the individual phase current to suppress the torque ripple [8].

The DTC method is more prominent owing to the high-performance application since the stator flux amplitude is controlled at the knee point of the saturation curve [9]; however, the stator flux amplitude is not controlled in the DTC of the BLDC motor because we do not have its exact shape. In fact, sharp dips occur during commutations due to the effect of the freewheeling diode conduction [10].

Using a single current sensor in the DC-link was introduced to reduce the cost. In this strategy, the error of the DC-link current was passed through a PI controller to provide the duty cycle. This technique comes with a high average torque ripple in addition to a severe commutation torque ripple.

In this study, a high-performance direct DC-link current control (DDLCC) is applied to reduce the average torque ripples. Instead of the torque control, the DC-link current is controlled in the DDLCC method. In fact, the error of this current is passed through the hysteresis controller. The fast response of the DC-link current over the hysteresis band is the key factor in the reduction of the average torque ripples compared to the DTC method. This proposed method has a fast transient response as much as the DTC method due to applying six active voltage vectors. Besides, compared to the DTC method, this method can reduce the torque ripple between two consecutive commutations, lower the computational burden, guarantee a cost-effective drive, and increase reliability.

Sharp commutation torque ripple is the main problem of applying one current sensor to control the BLDC motors. In this context, a four-level hysteresis controller is utilized to distinguish the commutation intervals, and then, the commutation torque ripple is repressed by applying a proper single-switch conduction voltage vector. In other words, these vectors are applied at the beginning of each sector to unify the rise and fall times of two commutated currents and consequently suppress the commutation torque ripples. To provide a precise comparison, the simulation and experiment of both DTC and the proposed methods are scrutinized and compared.

II. BLDC Motor Model

The mathematical model in the stationary reference frame is usually utilized for the analysis of the BLDC motors since the voltage and current waveforms of this motor in non-sinusoidal, and cannot be transferred into the synchronous reference frame by the common Park

Transformation. Thus, the relation between the stator voltages ($v_{s\alpha}$ and $v_{s\beta}$), currents ($i_{s\alpha}$ and $i_{s\beta}$), and back-EMFs ($e_{s\alpha}$ and $e_{s\beta}$) can be represented as

$$\begin{cases} v_{s\alpha} = R_s i_{s\alpha} + L_s \frac{di_{s\alpha}}{dt} + e_{s\alpha} \\ v_{s\beta} = R_s i_{s\beta} + L_s \frac{di_{s\beta}}{dt} + e_{s\beta} \end{cases} \quad (1)$$

where R_s and L_s are stator resistance and inductance, respectively.

The stator and rotor flux linkages are estimated by (2) and (3).

$$\begin{aligned} \psi_{s\alpha} &= \int (v_{s\alpha} - R_s i_{s\alpha}) dt \\ \psi_{s\beta} &= \int (v_{s\beta} - R_s i_{s\beta}) dt \end{aligned} \quad (2)$$

$$\begin{aligned} \psi_{r\alpha} &= \psi_{s\alpha} - L_s i_{s\alpha} \\ \psi_{r\beta} &= \psi_{s\beta} - L_s i_{s\beta} \end{aligned} \quad (3)$$

In practice, however, a low pass filter (LPF) has been used instead of integration to remove the DC offset created by the sensors.

Different torque estimations have been introduced in prior studies. Torque estimation plays a significant role in the direct torque control of the BLDC motor. In other words, inappropriate torque estimation is a source of both commutation and average torque ripples. Here, the following equation is used to obtain the simulation and experiments of all analyzed methods [2].

$$T = \frac{3P}{4}\left(\psi_{s\alpha}\, i_{s\beta} - \psi_{s\beta} i_{s\alpha}\right) \quad (4)$$

The torque is also computed by the DC-link current (i_{dc}) [10].

$$T = P\lambda_m i_{dc} \quad (5)$$

where P and λ_m, are the poles count and the flux produced by the magnet. As obvious, the DC-link current direction is permanently changed during a switching cycle from a negative value to a positive value. Therefore, the torque estimated by this technique contains switching frequency ripples.

III. DTC OF BLDC MOTOR

In the BLDC motor, the current is injected at the top flat portion of the phase-EMF to attain a constant torque. In this context, direct torque control of the BLDC motor is introduced (Fig. 2). Based on this topology, there exists merely one control loop. Table 1 shows the lookup table applied in [10] for the control of the BLDC motors. According to the vectors used in this table, the common-mode voltage problem is removed; however, the torque ripple is high by applying these vectors to the inverter, and the dead time needs to be adjusted in an inverter leg.

IV. PROPOSED DDLCC METHOD

In the DDLCC method, the torque control is substituted by the DC-link current control to lower the average torque ripple by the fast response around the hysteresis band. To suppress the commutation torque ripple by appropriate single-switch conduction vectors, the commutation intervals are first distinguished by a four-level hysteresis controller. Then, the sector-based conduction vector is applied to unify the rise and fall time of the commutated currents. Fig. 3 illustrates the control block diagram of the DDLCC strategy with a four-level hysteresis controller. The lookup table used in this strategy for counter-clockwise (CCW) and clockwise (CW) directions are tabulated in Tables 2 and 3, respectively. All vectors applied in these tables are as follows:

- $V_1 \triangleq (100001)$, $V_2 \triangleq (001001)$, $V_3 \triangleq (011000)$, $V_4 \triangleq (010010)$, $V_5 \triangleq (000110)$, $V_6 \triangleq (100100)$, $V_{01} \triangleq (100000)$, $V_{02} \triangleq (010000)$, $V_{03} \triangleq (001000)$, $V_{04} \triangleq (000100)$, $V_{05} \triangleq (000010)$, $V_{06} \triangleq (000001)$, $V_0 \triangleq (000000)$.

Where V_1 to V_6 are used between two consecutive commutations and represent two-phase conduction mode voltage vectors. In fact, only two phases are conducted in each sector with the same current amplitude but in the opposite direction. Moreover, V_{01} to V_{06} are merely utilized during commutations to suppress commutation torque ripple by unifying the fall time and rise time of two commutated currents. Furthermore, V_0 represents the zero vector where all IGBTs are off.

A. The Principle of the DDLCC Method

As mentioned, the torque control is substituted with the DC-link current control in the proposed method. In this context, the behavior of the torque and DC-link current are depicted in Fig. 4 for both DTC and proposed DDLCC methods. Similar points on each graph correspond to each other ((1-7) and (11-17)). As seen, the switches M1 and M2 are turned on (Fig. 5-a) when the torque passes the lower level of the hysteresis band (points 1 and 5 in Fig. 4-a). Consequently, both torque and DC-link current

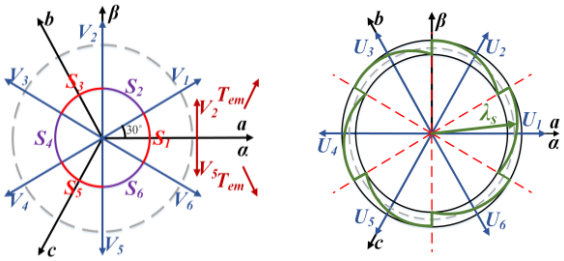

Fig. 1. Voltage space vectors, sectors, and stator flux trajectory (green curve) of BLDC motors.

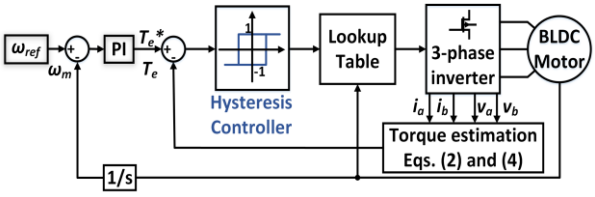

Fig. 2. Conventional DTC of the BLDC motor [10].

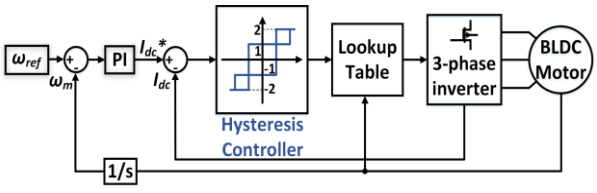

Fig. 3. Block diagram of the proposed DDLCC method.

TABLE I
LOOKUP TABLE USED IN [10]

e_T	S_1	S_2	S_3	S_4	S_5	S_6
1	V_2	V_3	V_4	V_5	V_6	V_1
-1	V_5	V_6	V_1	V_2	V_3	V_4

TABLE II
PROPOSED LOOKUP TABLE FOR CCW ($i_{dc}^* > 0$)

e_T	S_1	S_2	S_3	S_4	S_5	S_6
2	V_{06}	V_{03}	V_{02}	V_{05}	V_{04}	V_{01}
1	V_2	V_3	V_4	V_5	V_6	V_1
-1	V_0	V_0	V_0	V_0	V_0	V_0

TABLE III
PROPOSED LOOKUP TABLE FOR CW ($i_{dc}^* < 0$)

e_T	S_1	S_2	S_3	S_4	S_5	S_6
1	V_0	V_0	V_0	V_0	V_0	V_0
-1	V_5	V_6	V_1	V_2	V_3	V_4
-2	V_{04}	V_{01}	V_{06}	V_{03}	V_{02}	V_{05}

increase due to the phase current increment. That is, the phase current increment and ripple corresponds to the electromagnetic torque increment and ripple. In contrast, when the electromagnetic torque passes the upper level of the hysteresis band (points 3 and 7 in Fig. 4-a), M1 and M2 are consequently turned off, and accordingly, body diodes D3 and D6 turn on.

According to Fig. 5-b, the DC-link current direction has been reversed. Fig. 5 shows that a similar trend can be seen in both torque and DC-link current. That is, the DC-link current increases with a positive value when the torque increases, and the DC-link current is negative when the torque reduces. The negative value of the DC-link current is beneficial since it creates fast movement and changes over the hysteresis band. As expected, controlling the DC-link current can accordingly reduce the torque ripple by fast changes over the hysteresis band (Fig. 4-c).

The DC-link current and its reference in the DDLCC method are depicted in Fig. 4-d. Based on this Fig., the negative value of the DC-link current corresponds to the fast movement over the hysteresis band; hence, torque ripple reduction is guaranteed by direct DC-link current control.

It must be mentioned that the lookup table tabulated in Table I is applied in this analysis.

B. Commutation Torque Ripple Reduction

As already mentioned, the DC-link current control can reduce the torque ripple between two consecutive commutations; nonetheless, severe commutation torque ripple is inevitable. Various parameters can intensify the commutation torque ripple including DC-link voltage and stator inductance. During commutation intervals, one phase is completely ON, and two remaining phases are commutated. That is, one phase must be turned off and another one must be turned on. As the fall and rise times of the commuted phases are not identical, the third phase is distorted and consequently, the torque ripple is intensified. To suppress the commutation torque ripple, a four-level hysteresis band is applied to detect the commutation interval; next, since the fall time is usually longer than the rise time, the commutated phase, which must be turned on, must be permanently turned off and on to achieve a similar fall time and rise time. In this context,

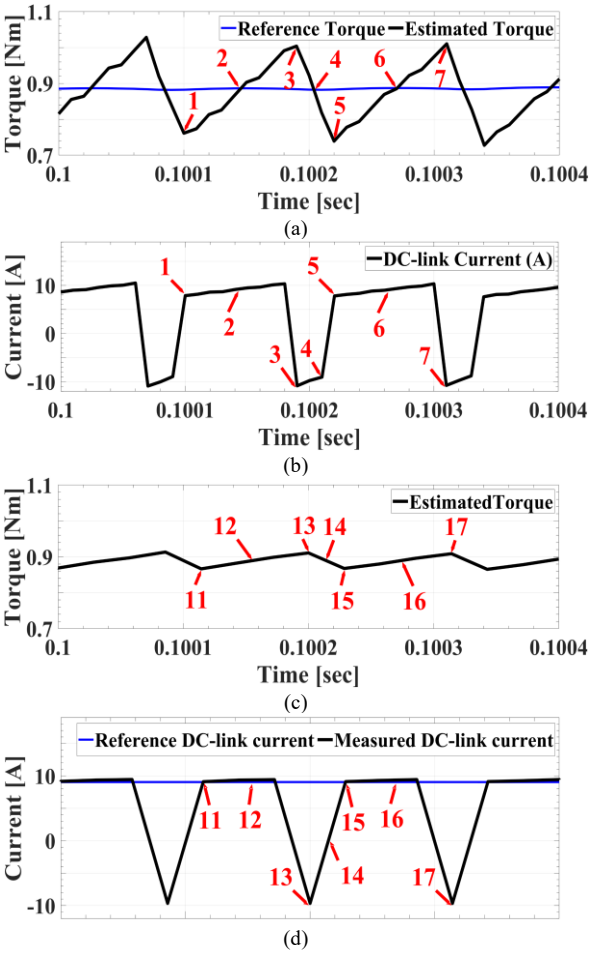

Fig. 4. Torque and current performance, (a) estimated and reference torque (DTC), (b) measured DC-link current (DTC), (c) estimated torque (DDLCC), (d) measured and reference DC-link current (DDLCC).

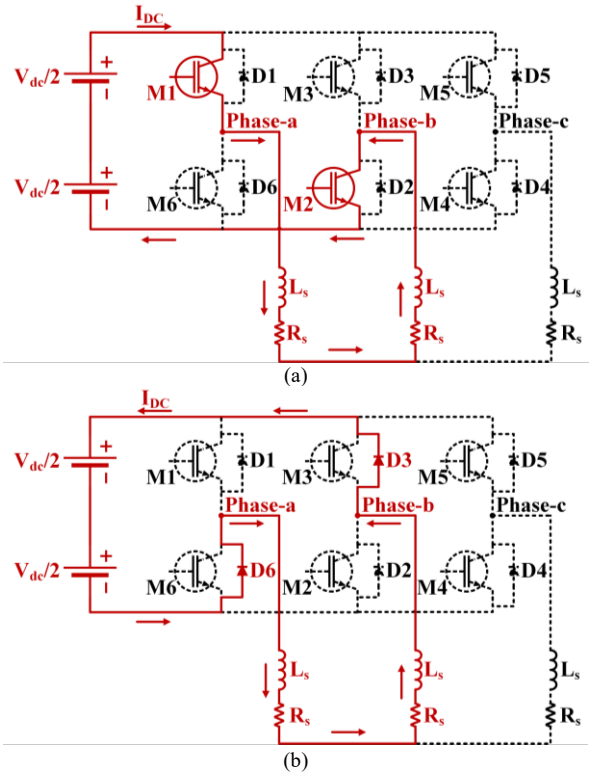

Fig. 5. (a) M1 and M2 are ON, and (b) D3 and D6 are ON.

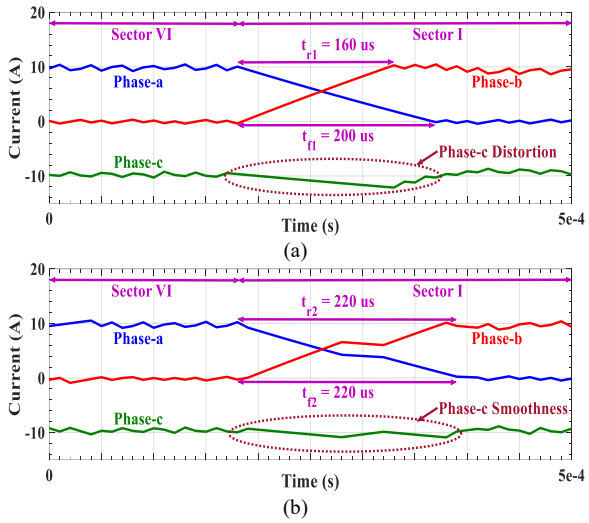

Fig. 6. Three-phase currents: (a) without applying the proper vector, (b) with applying the proper vector.

single-switch conduction vectors must be applied. In fact, one IGBT is ON, and five IGBTs are OFF. Fig. 6 shows the performance of two commutated phases without and with applying appropriate sector-based conduction vectors (Tables II and III).

V. Experimental Results

The performance of both DTC and DDLCC methods is evaluated in this section. Fig. 7 shows the test bench utilized for experiments. The motor specifications are also tabulated in Table IV. In order to provide a comparison, the experimental results are performed for both DTC and proposed DDLCC. By applying the step load change from no load to the rated load, the performance of both control methods is investigated (Figs. 8 and 9). As indicated, the actual motor speed follows its reference in both methods (Figs 8-a and 9-a). In addition, Fig. 8-b indicates the torque follows its command in the DTC method. The torque reference is generated by passing the speed error through a PI controller. In this DDLCC method, however, the torque equals the load torque (Fig. 9-b) since the DC-link current is controlled instead of the torque. In fact, the DC-link current reference is generated by passing the speed error through a PI controller. As demonstrated in Figs. 8-b and 9-b, the torque ripple of the DDLCC is much lower than that of the DTC. Figs. 8-c and 9-c indicate that the current ripple has a direct relation to the torque ripple. In other words, any technique that can reduce the torque ripple can reduce the current ripple as well.

To provide a numerical analysis, the torque ripple T_{rip} is calculated by this equation [11, 12].

$$T_{rip} = \sqrt{\frac{1}{N}\sum_{i=1}^{N}(T_{e-error}(i))^2} \times 100 \qquad (6)$$

where $T_{e-error}(i)$ is the discrepancy between the reference torque and the estimated torque, and N is the predetermined sample numbers. The numerical analysis shows the proposed DDLCC method with a 3.34 % torque ripple reduces the torque by about 58% compared to the DTC method (7.93 % torque ripple).

TABLE IV
Motor Specifications

$P_n = 120\ [W]$	$V_{DC} = 33\ [V]$	$R_s = 0.218\ [\Omega]$
$L_s = 264\ [mH]$	$\lambda_m = 0.0188\ [Wb]$	$\omega_m = 1300\ [rpm]$
$P = 8$	$T_n = 0.89\ [N.m]$	$Eff. = 69.43\ [\%]$

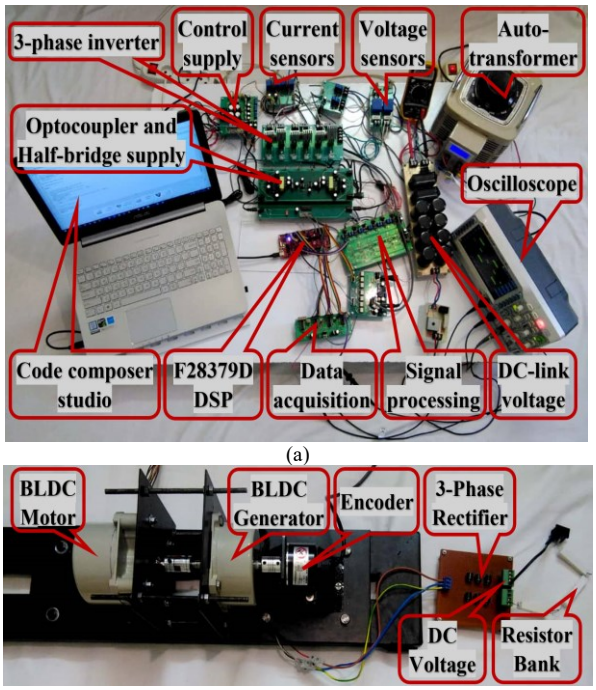

Fig. 7. The test bench utilized for experiments: (a) control side and (b) motor side.

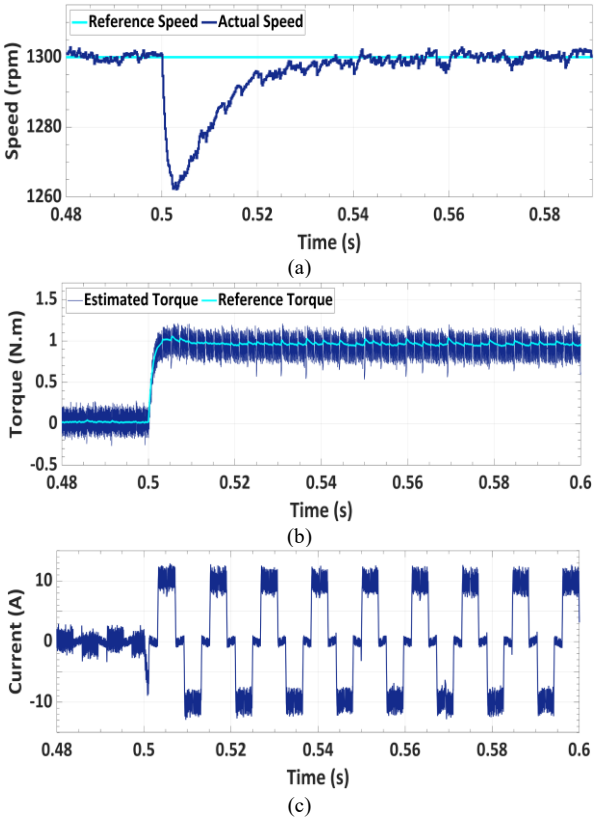

Fig. 8. Experimental results of the DTC method: (a) reference and estimated speed, (b) reference and estimated torque, (c) phase-a current.

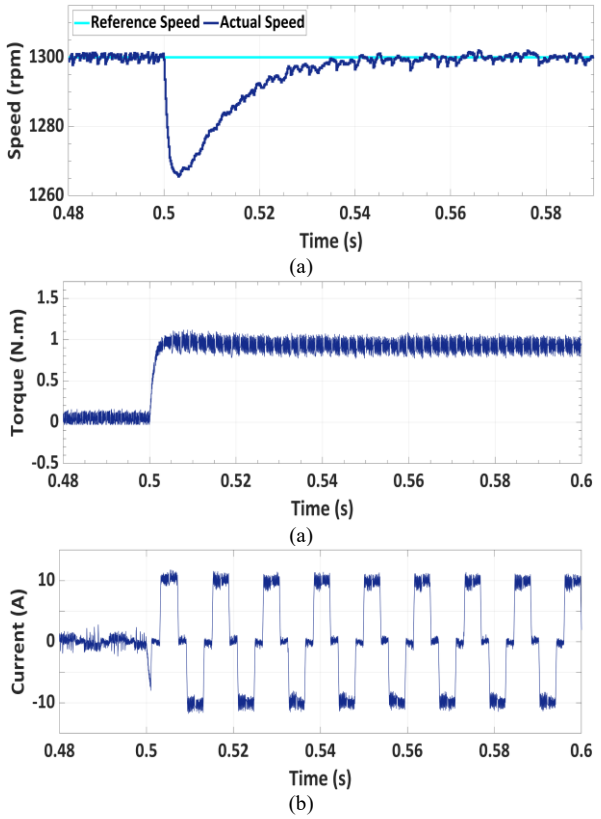

Fig. 9. Experimental results of the proposed DDLCC method: (a) reference and estimated speed, (b) estimated torque, (c) phase-a current.

VI. Conclusion

In this research, a low-cost direct DC-link current control (DDLCC) method is utilized to efficiently reduce the average torque ripples compared to the DTC method. The proposed method has a fast dynamic torque response similar to the DTC method; however, the computational burden is decreased, the control block is simplified, and the reliability is increased. Next to this, single-switch conduction voltage vectors are applied to suppress the commutation torque ripples. These vectors are only applied during commutations distinguished by the multilevel hysteresis controller. Experimental results confirm the effectiveness of the proposed DDLCC method with a multilevel hysteresis controller and appropriate voltage vectors.

Acknowledgment

This research was supported by Basic Science Research Program through the National Research Foundation of Korea (NRF) funded by the Ministry of Education (2020R1G1A1012756 & 2018R1D1A1B0704373514).

References

[1] A. Halvaei Niasar, A. Vahedi and H. Moghbelli, "A Novel Position Sensorless Control of a Four-Switch, Brushless DC Motor Drive Without Phase Shifter," *IEEE Transactions on Power Electronics*, vol. 23, no. 6, pp. 3079-3087, Nov. 2008.

[2] R. Heidari, G. A. Markadeh, and S. Abazari, "Direct torque and indirect flux control of brushless DC motor with non-sinusoidal back-EMF without position sensor," *19th Iranian Conference on Electrical Engineering (ICEE)*, Tehran, pp. 1-5, 2011.

[3] R. Heidari and J. -W. Ahn, "Torque Ripple Reduction of BLDC Motor with a Low-cost Fast-response Direct DC-link Current Control," *IEEE Transactions on Industrial Electronics*, doi: 10.1109/TIE.2023.3247732.

[4] Yanxin Li, Zi Qiang Zhu, and Guang Jin Li, "Influence of Stator Topologies on Average Torque and Torque Ripple of Fractional-Slot SPM Machines with Fully Closed Slots," *IEEE Trans. on Industry Applications*, vol. 54, no. 3, June 2018.

[5] R. Heidari, J. -W. Ahn, D. -H. Kang and K. -I. Jeong, "A Loss Reduction of Dual Air-gap Surface-mounted Permanent Magnet Synchronous Motor," *2022 25th International Conference on Electrical Machines and Systems (ICEMS), Chiang Mai*, Thailand, 2022, pp. 1-5.

[6] V. Viswanathan and J. Seenithangom, "Commutation Torque Ripple Reduction in the BLDC Motor Using Modified SEPIC and Three-Level NPC Inverter," *IEEE Trans. on Power Elect.*, vol. 33, no. 1, Jan. 2018.

[7] M. Masmoudi, B. El Badsi, and A. Masmoudi, "Direct Torque Control of Brushless DC Motor Drives with Improved Reliability," *IEEE Trans. on Industry Applications*, vol. 50, no. 6, Nov.-Dec. 2014.

[8] S. K. Chari, R. Dhiman and R. Saxena, "Novel and Robust Hysteresis Current Control Strategies For a BLDC Motor: A Simulation Study and Inverter Design," *2018 2nd IEEE International Conf. on Power Electr.*, Intelligent Control and Energy Systems (ICPEICES), pp. 841-846, 2018.

[9] M. H. Soreshjani, R. Heidari, and A. Ghafari, "The Application of Classical Direct Torque and Flux Control (DTFC) for Line-Start Permanent Magnet Synchronous and its Comparison with Permanent Magnet Synchronous Motor," *Journal of Electrical Engineering and Technology*, Vol. 9, no. 6, pp. 1954-1959, 2014.

[10] S. B. Ozturk, H. A. Toliyat, "Direct Torque Control of Brushless DC Motor with Non-sinusoidal Back-EMF," *IEEE International Electric Machines & Drives Conf.*, vol. 1, pp. 165-171, 2007.

[11] R. Heidari, "Model predictive combined vector and direct torque control of SM-PMSM with MTPA and constant stator flux magnitude analysis in the stator flux reference frame," *IET Electric Power Applications*, vol. 14, no. 12, pp. 2283-2292, Sep. 2020.

[12] S. A. Mansouri, A. Ahmarinejad, M. S. Javadi, R. Heidari, and João PS Catalão, "Improved double-surface sliding mode observer for flux and speed estimation of induction motors," *IET Electr. Power Appl.*, vol. 14, no. 6, pp. 1002-1010, June 2020.